

Technical Support Document for
Circumferential Cracking ARC
Non-Proprietary Version
Volume 1: Structural Analysis Model and
Integrated Burst Pressure Data Base



WARNING:
Please read the Export Control
and License Agreement on the
back cover before removing the
Wrapping Material.

Technical Report

**CIRCUMFERENTIAL CRACKS IN STEAM GENERATOR
TUBES: STRUCTURAL ANALYSIS MODEL AND
INTEGRATED BURST PRESSURE DATA BASE**

EPRI Final Report TR-107618

Volume 1

December 1997

Licensable Material

NOTICE: This report contains proprietary information that is the intellectual property of EPRI. Accordingly, it is available only under license from EPRI and may not be reproduced or disclosed, wholly or in part, by any Licensee to any other person or organization.

Prepared by
Tetra Engineering Group, Inc
110 Hopmeadow Street, Suite 800
Weatogue, CT. 06089

Prepared for
Electric Power Research Institute
3412 Hillview Avenue
Palo Alto, Ca 94304

EPRI Project Manager
D.A. Steininger
Steam Generator Management Program
Nuclear Power Group

DISCLOSURE

This report has not been reviewed to determine whether it contains patentable subject matter, nor has the accuracy of its information or conclusions been evaluated. Accordingly, the report is not to be considered a published report and is not available for general distribution, and its distribution is limited to employees and advisors of EPRI for the sole purpose of evaluating the progress and future course of the project described in the report. Until the report has been reviewed and evaluated by EPRI, it should be neither disclosed to others nor reproduced, wholly or partially, without written consent of EPRI.

Table of Contents

1 INTRODUCTION	4
2 ANALYTICAL MODEL	5
2.1 Morphology	5
2.2 Bending Case	6
2.2.1 Methodology	6
2.2.2 Load Equilibrium	9
2.3 Limit Cases	11
2.3.1 Axial Bursting	12
2.3.2 Tensile Failure	12
2.4 Flow Stress Coefficient	13
3 LATERAL RESTRAINT EFFECT	15
3.1 Phenomenology	15
3.2 Experimental Data	16
3.3 Dependence on Stiffness	17
3.4 Influence of Support Offset	19
4 RESULTS OF STRUCTURAL ANALYSES	20
4.1 Tables and figures	20
4.1.1 Free Bending	21
4.1.2 Restrained Bending	23
4.2 Sample calculations	26
4.2.1 Manual calculations	26
4.2.2 Use of tables	27
4.3 Comparison to the Case of Axial Cracks	27
4.4 Comparison to Similar Studies	29
4.4.1 Free Bending	29
4.4.2 Restrained Bending	29
4.4.3 Limit Cases	31
4.4.4 Conclusions	31
5 BURST TESTING PROCEDURES	32
5.1 Laboratory Practices	32
5.2 Recommended Procedures	33
5.3 Load Index Values	33

5.4 Other Testing Procedures	34
6 EXPERIMENTAL VALIDATION	35
6.1 Belgian Data	35
6.1.1 Testing Conditions	35
6.1.2 Load Index	36
6.1.3 Free Bending	36
6.1.4 Restrained Bending	38
6.1.5 Tensile Loading	40
6.2 Millstone Data	42
6.2.1 Testing Conditions	42
6.2.2 Load Index	43
6.2.3 Free Bending	43
6.2.4 Restrained Bending	46
6.3 Westinghouse Data	48
6.3.1 Testing conditions	48
6.3.2 Load Index	49
6.3.3 Free Bending	49
6.3.4 Restrained Bending	51
6.4 ANO-2 Data	54
6.4.1 Testing Conditions	54
6.4.2 Load Index	55
6.4.3 Data	55
6.5 Framatome Data	57
6.5.1 Testing Conditions	57
6.5.2 Load Index	58
6.5.3 Free Bending	58
6.5.4 Restrained Bending	60
6.6 EDF Data (Pulled Tubes)	61
6.7 Conclusions	61
6.7.1 Free Bending	61
6.7.2 Restrained Bending	62
6.7.3 Validation	63
7 PROPOSED SGDSM IMPLEMENTATION	64
7.1 Generic approach	64
7.2 Alternate Repair Limit	68
7.2.1 Structural limit	69
7.2.2 Repair Limit	70
7.3 Tube Rupture Probability	71
7.4 Accident Leak Rate	71
7.5 Plant Specific Approach	71
7.6 Comparison to the Empirical Correlation Approach	72
8 MODEL CONSERVATISM	74
8.1 Thin Wall Approximation	74
8.2 Defect Morphology	74
8.2.1 Shape of Degraded Area	74
8.2.2 Out of Plane Components	75

8.2.3 Leakage Correlation	75
8.3 Restraint Configuration	75
8.4 Pressure Load on Flaw Lips	75
8.5 Ligaments in Crack Lips	76
8.6 Failure Stress in Tensile Mode	77
9 OVERALL COMPARISON WITH BURST DATA	78
10 UTILITY GUIDANCE	81
10.1 Structural Limit	81
10.1.1 Generic Approach	82
10.1.2 Specific Approach	84
10.2 Repair Limit	85
10.3 Detailed Condition Monitoring	85
11 SUMMARY AND CONCLUSIONS	87
REFERENCES	89
APPENDIX A - DEVELOPMENT AND RESOLUTION OF EQUATIONS	91
A1 Equilibrium Equations	91
A2 Analytical Resolution	92
A3 Numerical Resolution	93
A4 Calculation Results	94
A5 Specificity of EDM flaws	94
APPENDIX B - LATERAL RESTRAINT STIFFNESS	107
B1 Scope	107
B2 Beam Model	107
B3 Subcase 1	108
B4 Subcase 2	109
B5 Combined Case	109
B6 Single Lateral Restraint	110
B7 Flaw Located at Mid Span	110
B8 Tube Clamping in Second Lateral Restraint	111

1 INTRODUCTION

This report defines a structural analysis method for assessing the residual strength (burst capability) of Steam Generator (SG) tubes affected by circumferential cracking. The structural analysis considers the total degraded cross-sectional area as the governing parameter and redistributes this area in the most conservative manner. The analysis takes into account the tube lateral restraint provided by the adjacent tube sheet and support(s). It also considers the effect of the pressure load on the crack lips for SG accident conditions and the restraining load from local foil reinforcement for laboratory testing conditions.

This model is an improved version of that already described in EPRI report NP-6626 (ref. 5). Available burst data from various sources are compiled in order to validate the analytical model.

Applications of the analytical model and methodology should be differentiated between:

1. structural expertise of specific morphologies, using the full modeling capabilities, and
2. Steam Generator Defect Specific Management (SGDSM) implementation, for which a simplified conservative approach is recommended.

2 ANALYTICAL MODEL

2.1 Morphology

The circumferential flaw morphologies considered in the present report are subject to the following simplification: the tube periphery is affected by two flaws, each having a uniform depth penetration, from 0 to 100 % of the tube nominal thickness.

Typical morphologies complying with this definition are illustrated by figure 1.

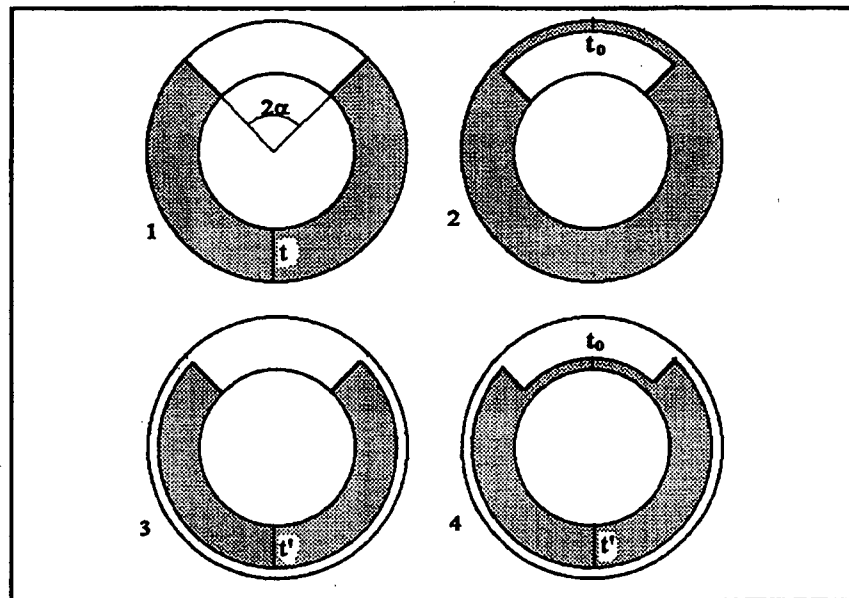


FIGURE 1: Assumed morphologies

Sketch 1 shows a single 100 % Through-wall Deep (TWD) flaw, of angular length 2α , in a tube with nominal wall thickness t . Sketch 2 is similar but shows a remaining ligament of thickness t_0 on the tube OD (case of PWSCC). The ligament could also be considered on the ID side (case of ODSCC).

Sketch 3 shows two flaws, of which the main flaw is 100% TWD while the other one reduces the remaining part of the tube circumference to a ligament thickness t' . Sketch 4 is similar but the "main" (i.e. deepest) flaw has a remaining ligament thickness t_0 . Sketches 3 and 4 illustrate a case of ODSCC but could be redrawn for PWSCC.

The flawed portion of the tube cross section (non shaded area of the sketches) is usually called the Percent Degraded Area and is designated by PDA.

While the present report will fully address these simple morphologies, the same methodology could be extended to more complex cases, in a way similar to that indicated in ref. 3.

With reference to real crack morphologies, as observed by destructive examination of tubes pulled from steam generators, the degraded areas can be approximated by the uniform depth model. This also implies integrating in a single plane crack components that actually lie at slightly axial offset locations and may neglect the residual strength of the interconnecting ligaments. This is why the burst strength or real circumferentially degraded tubes can be significantly larger than predicted by any analytical tool.

2.2 Bending Case

2.2.1 Methodology

The configuration of a steam generator tube with a localized circumferential crack is shown in figure 1. The tube is internally pressurized until failure. Failure is considered to occur at the onset of unstable crack growth.

The net section collapse load criterion (ref. 1 to 3) is used to define the failure condition in the tube cross section containing the circumferential crack. This criterion was selected due to the ductile nature and inherent toughness of Inconel alloy 600 tube material. The net section collapse load criterion assumes a rectangular distribution of stresses equal to the material flow stress, σ_f , at the point of failure. Only pressure loading is considered on the tube as other "primary" type loads (as categorized in ASME Code terminology), such as seismic or vibration effects, are negligibly small in the vicinity of the SG tube sheet. In the crack segment, we consider that the crack lips are additionally loaded by either:

- the presence of a metal ligament within the 2α crack, also assumed at the flow stress (case A).
- an axial restraining load from the metal foil used as a local reinforcement of the plastic bladder in laboratory burst test conditions (case A).
- the fluid pressure (or a fraction thereof), as would be expected under SG service conditions (case B).

Figure 2 illustrates the distribution of stresses (tensile and compressive) for the two cases. When compared to the case of a 100% through wall crack, with no load on the crack lips, case A results in a higher burst pressure while case B results in a lower burst pressure. For both cases, the load on crack lips is considered as an

equivalent stress σ_{eq} , uniformly applied to the full wall thickness t , over the entire crack length.

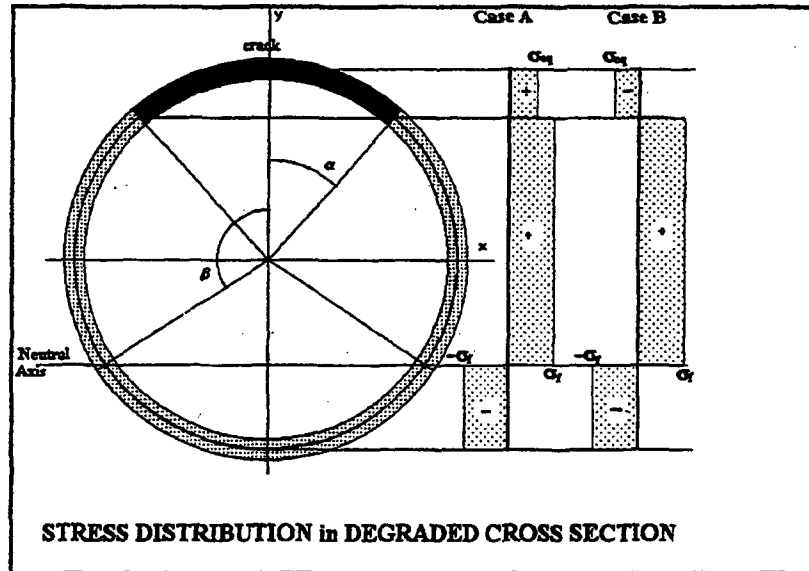


FIGURE 2: Assumed stress distribution in degraded cross section

For the various crack lips loads, the value of the "equivalent stress" is given by the following table:

TABLE 1: Equivalent stress

In the following sections of this report a distinction will be made between the "material ligament" case, directly characterized by the t_0/t ratio, and the two other "pressure type" cases, more conveniently characterized by the "load index" η .

When a lateral restraint is provided, such as by a flow distribution baffle (FDB), a tube support plate (TSP) or an egg crate (EC), an opposing moment is developed in the tube as illustrated by figure 3. The flaw is usually assumed to be located near the Top of Tube Sheet (TTS). This is the case of most practical interest but does not constitute a model limitation; for instance, a case of mid span crack location (between TTS and FDB) is also considered.

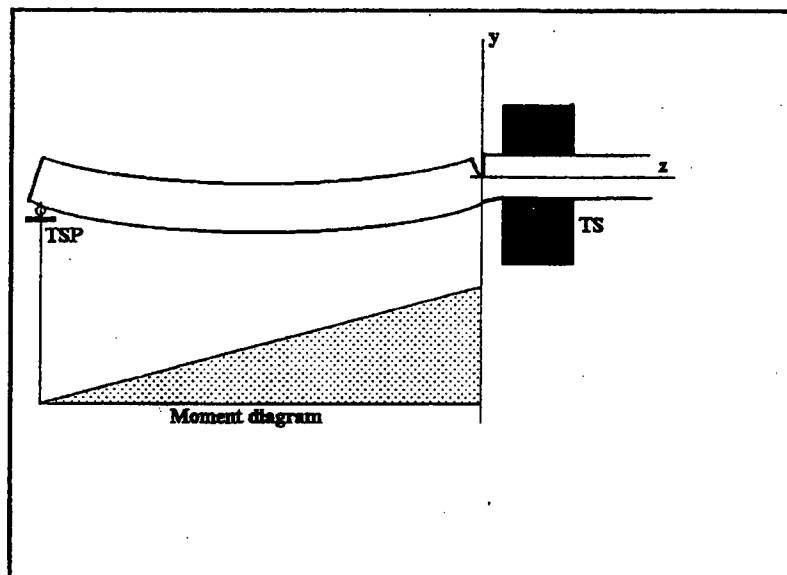


FIGURE 3: Model of lateral restraint

It should be noted that equation 2 is an approximation for the stress behavior at the crack location. It assumes a regular stress pattern in the full tube cross section, which is only restored at a short distance away from the crack location. The empirical factor k accounts also for this approximation.

2.2.2 Load Equilibrium

If no lateral restraint is provided (free bending), the term enclosed by a dotted box at the end of the equation 14 is excluded.

These equations allow to calculate the burst pressure of a tube with a circumferential crack 2α . 2α can also be considered the critical crack length for a tube with a differential pressure equal to p_{burst} .

$$\sigma = p_{burst} (R/t - 1)/2$$

The two equations can be solved for two unknowns (either P_n and β , or α and β), as a function of the given parameter (α or P_n). Thus, for any set of t_0/t and t'/t , the burst pressure can be determined as a function of the given crack length (2α) or, conversely, the critical crack length can be determined as a function of the given differential pressure.

Note that in all equations the crack angles must be expressed in radian; degree units may be used if π is replaced by 180.

Detailed calculations and results are provided in appendix A.

2.3 Limit Cases

Steam generator tubes with circumferential flaws will fail in a manner where the circumferential bending mode controls only when the flaw size is between two extremes. If the flaw size is small, the tube will fail by an axial oriented burst at a pressure consistent with an unflawed tube. With a large enough flaw, the tube will fail circumferentially in a manner consistent with a tensile overload. These two extremes are the limiting cases for the circumferential bending mode failure described in the previous Section and are discussed below.

2.3.1 Axial Bursting

For a "short" defect, failure occurs in the axial direction, either outside the defective area or initiated by a small axial component of the circumferential flaw. The transition of the axial burst behavior to a circumferential burst behavior occurs when the predicted burst pressure becomes equal to that of an unflawed tube. The latter value has been experimentally (ref. 6) shown to be given by:

2.3.2 Tensile Failure

For a "long" defect, tensile failure occurs if the applied axial force reaches the tensile resistance of the degraded cross section.

2.4 Flow Stress Coefficient

The flow stress coefficient $\sigma_f/(\sigma_u+\sigma_y)$ depends only on the tube material and the usual value of 0.5 is used in the present analysis.

In Section 2.3.2, the issue of selecting the proper flow stress coefficient $\sigma_f/(\sigma_u+\sigma_y)$ under dominantly tensile load was discussed. If the flaw is asymmetric (single 100% through-wall segment), the remaining ligament fails at a stress value close to the conventional σ_u . If the flaw is symmetric or uniformly degraded outside of the main through-wall flaw, ductile deformation will be restrained and failure may occur at a stress value getting close to yield when the relative ligament thickness becomes very small.

3 LATERAL RESTRAINT EFFECT

3.1 Phenomenology

Figure 4 illustrates the overall behavior of a tube, with a 100% through-wall circumferential flaw near the top of tube sheet, when the bending deflection is restrained by a lateral support. This Section summarizes actual observations during a laboratory test program (ref. 5). The 5 sketches show the condition of the tube as pressure is increased.

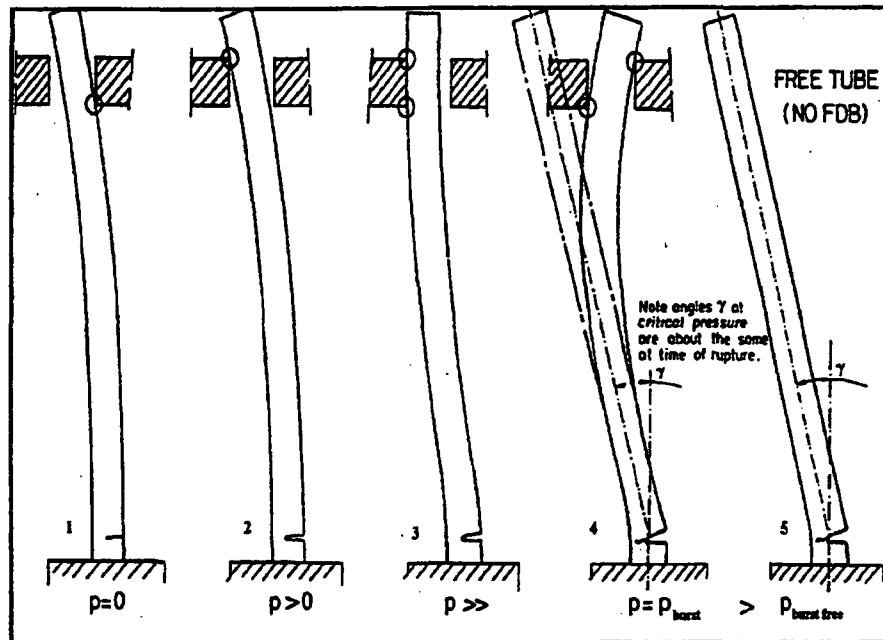


FIGURE 4: Progressive deformation of a pressurized tube

Sketch 1 shows the initial no pressure condition. A support lateral offset is assumed in the direction that tends to open the flaw.

Sketch 2 shows the tube as it is initially pressurized. The support contact point moves from one side to the opposite side.

In sketch 3, the pressure is increased. The tube deforms in the direction opposite of the initial direction (reverse bending). At one instant, the tube is vertical at the support level.

In sketch 4, the pressure reaches the burst value, P_{burst} . At this point the tube is likely to be in contact with both sides of the support. The large angular deformation, γ , at the flaw level initiates blunting of the crack tip and a Crack Tip Opening Displacement (CTOD). When the CTOD reaches a critical value, which is a constant and characteristic of the tube material and thickness, burst is initiated by unstable crack extension at the flaw tips. The value of the angular deflection, γ , is observed to be about the same as that for a tube in free bending (sketches 4 and 5). However, the burst pressure is much higher for the case of lateral restraint.

3.2 Experimental Data

Lateral restraining forces have been measured in a series of tests on 3/4" tubes with simulated TSP and/or FDB (ref. 5). Flaw lengths were 270° and 300° and some FDB supports were installed with offsets up to 20 mm (0.8"). The results are summarized in table 2.

TABLE 2: Restraining load measurement

¹ FDB and TSP are located at respectively 0.15 and 0.9 m from TTS

² Product of measured force by support distance from TTS ; for the double support configuration, the force is measured at FDB and the product is further divided by 1.1 (cf. Appendix B5 , Equation B-16)

TABLE 3: Stiffness index measurement

3.3 Dependence on Stiffness

TABLE 4: Correlation between κ and S(stiffness)

FIGURE 5: Influence of support configuration (stiffness)

TABLE 5: Formulation of Stiffness S

3.4 Influence of Support Offset

effect of initial load is wiped out by further tube deformation before the burst pressure is reached.

This does not mean that such offsets are innocuous. The corresponding secondary stresses may severely enhance both initiation and propagation of stress corrosion cracking. Examples are known (Ringhals 4 plant) where the location and orientation of circumferential SCC at the periphery of the tube sheet clearly indicated the detrimental effect of tube bending due to interference with the FDB.

4 RESULTS OF STRUCTURAL ANALYSES

4.1 Tables and figures

Tables of the normalized burst pressure (in appendix A) have been prepared for the case $R/t = 8.24$ (Westinghouse SG design) or $R/t=7.31$ (Combustion Engineering SG design) and the following configurations or typical values of relevant parameters:

PDA from 0 to 100 %, in 5% increments

Flaw morphologies

- Through-wall, in free and restrained ($\kappa= 0.6, 0.7, 0.8,$ and 0.9) bending, for $\eta = -1, -0.5, 0, 0.5, 1$ and 1.5 (tables A1 to A5)
- Partial penetration, in free and restrained ($\kappa= 0.6, 0.7, 0.8,$ and 0.9) bending, for $t_0/t = 0.1, 0.2$ and 0.3 (tables A6 to A10)
- Symmetrical, for $\eta = -1$ and 0 (table A11)

The neutral axis location (angle β) is not reported because it is of no practical interest; it is typically within a relatively narrow range of 160 to 180° for restrained bending.

The figures in this Section apply to both Westinghouse ($R/t = 8.24$) and Combustion Engineering ($R/t = 7.31$) design, as the differences are not visually distinguishable.

4.1.1 Free Bending

Numerical results are given in tables A1 and A6. Figures 6 and 7 illustrate the normalized burst pressure as a function of PDA, for various values of the load on the flaw lips, η , and relative ligament thickness between the flaw lips, t_0/t . The latter figure is also duplicated as a function of the flaw length (Fig. 8).

Fig. 6 shows the major influence of loads applied to flaw lips. This explains the large difference that may exist between SG service conditions ($\eta < 0$) and some laboratory testing conditions ($\eta > 0$).

FIGURE 6: Normalized burst pressure as a function of PDA, for $t_0 = 0$, $R/t = 7.31$ and a load index in the range of -1 to +1.5

FIGURE 7: Normalized burst pressure as a function of PDA, for $\eta = 0$, $R/t = 8.24$ and a ligament thickness t_0 in a range of 0 to 30 % of the nominal tube wall thickness

FIGURE 8: Normalized burst pressure as a function of flaw length, for $\eta = 0$, $R/t = 8.24$ and a ligament thickness t_0 in a range of 0 to 30 % of the nominal tube wall thickness

4.1.2 Restrained Bending

Numerical results are given in tables A2 through A5, for TWD flaws, and A7 through A10 for partial penetration flaws. Figures 9 to 11 illustrate the normalized burst pressure as a function of PDA, for various values of the stiffness index κ (for $\eta = t_0/t = 0$), the load index η (for $t_0/t = 0$ and $\kappa = 0.6$) and the relative ligament thickness t_0/t (for $\eta = 0$ and $\kappa = 0.6$). The latter figure is also duplicated as a function of the flaw length (Fig. 12).

Fig. 9 indicates that restrained bending results in much higher burst pressures than free bending. In addition, this figure shows the significant influence of the restraint configuration (stiffness index κ) on the burst pressure.

Fig. 10 shows the major influence of loads applied to flaw lips. This explains the large difference that may exist between SG service conditions ($\eta < 0$) and some laboratory testing conditions ($\eta > 0$).

Comparison of Fig. 11 and 12 indicates less sensitivity to ligament thickness when the burst pressure is plotted as a function of PDA. The burst pressure may even be higher without ligament, in the tensile failure mode, because of the assumed "notch effect" on the flow stress.

FIGURE 9: Normalized burst pressure as a function of PDA, for $t_0/t = 0$, $\eta = 0$, $R/t = 8.24$ and a stiffness index in a range of 0.6 to 0.9 (+ free bending)

FIGURE 10: Normalized burst pressure as a function of PDA, for $t_0/t = 0$, $\kappa = 0.6$, $R/t = 8.24$ and load index in a range from -1 to +1.5

FIGURE 11: Normalized burst pressure as a function of PDA, for $\eta = 0$, $\kappa = 0.6$, $R/t = 8.24$ and ligament thickness t_0 in a range of 0 to 30 % of tube wall nominal thickness

FIGURE 12: Normalized burst pressure as a function of flaw length, for $\eta = 0$, $\kappa = 0.6$, $R/t = 8.24$ and ligament thickness t_0 in a range of 0 to 30 % of tube wall nominal thickness

4.2 Sample calculations

4.3 Comparison to the Case of Axial Cracks

Figure 13 compares the burst pressure of axial and circumferential flaws. Flaws are considered 100 % through-wall with lengths ranging from 0 to 55 mm. The 7/8" diameter tube ($t=0.05"$) is considered to have lower bound high temperature material properties ($\sigma_u + \sigma_y = 125$ ksi).

For the axial flaw, the burst equation is taken from ref. 6 and applies to free span. For the circumferential flaw, the burst pressure calculation presented in Section 2 is used with $\kappa=0.6$ and $\eta=-0.5$.

It can be seen that the burst pressure is much higher for the circumferential crack. For the reference pressure of 3 times normal operating pressure, 4380 psi (normalized to $P_n = 0.289$), the structural limit is almost 4 times larger than that for an equivalent length axial crack.

FIGURE 13: Comparison of the burst strength of axial and circumferential cracks

4.4 Comparison to Similar Studies

Only one analytical study of circumferential flaws in SG tubes was found to be documented in the available literature. EPRI report NP-6865-L (ref. 7) describes the approach used in France by EDF and Framatome.

4.4.1 Free Bending

The collapse load approach is used for through-wall flaws. No consideration is given to degradation outside the main flaw ($t'/t = 1$), ligament in the main flaw ($t_0/t = 0$) or "pressure type" load on the flaw lips ($\eta = 0$). The expression used for the burst pressure is identical to equation A-22. The flow stress coefficient is taken equal to 0.5 but a 20 % higher value is also considered to provide an improved empirical fit to laboratory test data (see Section 6.5.3).

4.4.2 Restrained Bending

The collapse load approach is used again, with a beam model to account for the lateral restraint. However the required parametric adjustment (equivalent to the "stiffness index" κ) is obtained from a Finite Element Model (FEM) tube analysis instead of a direct measurement of the restraining moment.

The only case described refers to a single lateral support (at 150 mm = 6" from TTS) with full rotational restraint and a 100%TWD flaw located at mid span. The results are illustrated graphically for either no pressure or full pressure on the flaw lips. These French results have been scaled and normalized in figure 14 to allow comparison with the methodology of this report (based on a stiffness index $\kappa = 0.68$, corresponding to a value $S_{eq} = 1/a = 6.7 \text{ m}^{-1}$, in accordance with equation 36 and table 5). It can be seen that the agreement is very good.

FIGURE 14: Comparison between restrained bending analyses

4.4.3 Limit Cases

4.4.4 Conclusions

The French approach is very similar to that proposed in the present report. Based on the information presented in ref. 7, it does not however provide the same flexibility to account for support configuration (stiffness index κ) and loads acting on the flaw lips (ligament and load index η).

5 Burst Testing Procedures

Experimental burst data provide the validation basis for any structural model. It is therefore necessary to ensure that the data points are produced under well defined, acceptable testing conditions. This Section provides a short summary of a dedicated study reported in Reference 4.

5.1 Laboratory Practices

While most laboratories have realized that the simple use of a thin plastic bladder does not allow to achieve true burst of through-wall flaws, the lack of testing guidelines led them to develop their own individual mitigating practices on an empirical basis. The use of a thicker bladder, when coupled with a high pressurizing rate, is sometimes sufficient but a reliable solution requires some kind of local reinforcement, generally in the shape of a thin metallic foil bridging the flaw, between the bladder OD and the tube ID. Large variations are observed in the selected foil characteristics:

- **Material:** material commonly used is copper, brass or steel, with a tensile strength ranging from 300 MPa (43 ksi) to 1200 MPa (170 ksi).
- **Dimensions** (for circumferential flaws): in the circumferential direction, the foil spans the flaw length but may extend up to the full tube circumference. In the axial direction, the foil width may vary from a minimum value of 0.5" (12 mm) up to several inches.
- **Interface condition:** the interface between foil and tube may be dry, lubricated or bonded (by adhesives such as "loctite")

The load index associated with testing conditions needs to be known with sufficient accuracy to

- either provide a support to the structural analysis model
- or to allow a direct extrapolation to the SG service conditions (burst data adjustment).

Unfortunately not all procedures allow a reliable definition of the axial restraining load applied by the foil to the flaw lips.

5.2 Recommended Procedures

5.3 Load Index Values

5.4 Other Testing Procedures

Testing procedures not complying with the above recommendations may result in burst being triggered by foil tearing or incomplete extrusion. This leaves a significant uncertainty as to the value of η associated with burst (typically within a range from -0.5 to 1.5). No accurate burst data can be derived from such testing conditions, unless specifically qualified. Guidelines for alternate procedure qualification are provided in ref. 4.

6 EXPERIMENTAL VALIDATION

Experimental burst pressures are compared to their theoretical predictions in order to validate the structural model and analysis.

Measured values are associated with a symbol to identify the failure mode:

- C for circumferential failure
- A for axial failure
- ? for unreported failure mode
- > when true burst was not achieved, generally because of premature leakage.

Calculated values of the normalized burst pressure P_n are the lowest of 0.6, the bending value from Section 2.2 and the tensile value from Sections 2.3.2 and 2.4. The tensile value is discarded if the restraint configuration prevents a tube axial movement.

The ratio of measured to calculated value is used for comparison. Statistics (average and standard deviation of the ratio, regression line between measured and calculated values) are computed when meaningful (restrained bending).

6.1 Belgian Data

The Belgian burst test program for circumferential flaws was performed by Laborelec in 1982 through 1989 and was documented in EPRI report NP-6626 (ref. 5). The results of forty seven experimental tests are compared to the calculated values. The results are considered separately for free bending and supported configurations. In addition, eleven tensile tests from SG pulled tubes (1993 and 1994) are used to evaluate the flow stress coefficient applicable to circumferential flaws under axial loading.

6.1.1 Testing Conditions

The test specimens were manufactured from both 7/8" ($t = 0.05$ ") and 3/4" ($t = 0.043$ ") diameter tubes, with 100% through-wall flaws. The specimens were pressurized with a plastic bladder and local foil reinforcement to prevent leakage. In some cases, premature failure of the bladder/foil occurred and these pressure data are recorded as lower bound of the burst pressures. The corresponding underestimation is reasonably small as the testing procedure used was capable of

achieving true burst; this was further confirmed by CTOD measurements close to the critical value (ref. 5).

The flaws were located 1/4" above simulated tube sheet. Free bending was either allowed or prevented by lateral restraint.

Various test support configurations were used. The support configurations simulated were: a Flow Distribution Baffle (FDB) only at 150 or 500 mm from TTS, a Tube Support Plate (TSP) only at 900 or 1100 mm from TTS, and a combination of both FDB and TSP.

The support geometry consisted of a diametrical gap ranging from 0.8 mm (TSP) to 2 mm (FDB) and a series of lateral offsets of 0, 10 or 20 mm. The testing procedure complied with the intent of the EPRI burst test guidelines (ref. 8).

6.1.2 Load Index

6.1.3 Free Bending

TABLE 6: Belgian program - Free bending

FIGURE 15: Comparison of calculated and measured burst pressures in free bending (Belgian data)

6.1.4 Restrained Bending

TABLE 7: Belgian program - Restrained bending ($R/t = 824$)

FIGURE 16: Comparison of calculated and measured burst pressures in restrained bending (Belgian data)

6.1.5 Tensile Loading

Table 8 summarizes the tensile load results for 11 SG tubes pulled from the Belgian units Doel 4 (affected by circumferential ODSCC) and Tihange 3 (mainly affected by circumferential PWSCC). The load is computed from the degraded cross section area (PDA measured by visual examination) and the CMTR mechanical properties (YS and UTS) at room temperature and compared to the direct measurement. For some Doel 4 data, the mechanical properties were also measured by Laborelec on the pulled tubes, with slightly higher values than documented in the CMTR. The measured values were then used for calculation.

The results are illustrated by figure 17. A good agreement is observed and confirmed by the indicated slope and correlation coefficient of the regression line.

TABLE 8: Belgian program - Tensile tests

FIGURE 17: Comparison of measured and calculated tensile loads for degraded pulled tubes

6.2 Millstone Data

The results of the Millstone 2 Burst Test program on circumferential flaws are documented in a Northeast Utilities memo (ref. 8). The tests were performed by CE and Westinghouse in 1989 through 1991. Forty eight experimental data are compared to the calculated values. The results are considered separately for free bending and supported configurations. One test specimen (Y) was considered as an "outlier" by ref. 8 and is not included in the following review.

6.2.1 Testing Conditions

The test specimens were manufactured from 3/4" ($t = 0.048$ ") diameter tubes, with 100% through-wall flaws and partial penetration flaws. A plastic bladder and local foil reinforcement was used to prevent leakage from the through-wall flaw specimens. Partial penetration flaws were pressurized without a bladder and failure (ligament rupture) was observed without flaw length increase. The corresponding pressures were high enough to initiate circumferential burst of a 100% TWD flaw of the same length and do qualify as valid data points. The absence of length extension is due to the rapid depressurization caused by leakage and would have been avoided by the use of a simple bladder (without foil reinforcement).

For partial penetration flaws, the ligament thickness was measured after circumferential failure; heavy plastic deformation (thinning) of the ligament resulted in significant measurement uncertainty, as stated by the experimenters.

The flaws were located 0.003" to 1.0" above a simulated tube sheet. Free bending was either allowed or prevented by lateral restraint.

Various test support configurations were used. The support configurations simulated the presence of either the first egg crate support at 28.125" above TTS or the second egg crate support at 60.125" above TTS.

The testing procedure complied with the intent of the EPRI burst test guidelines (ref. 8).

6.2.2 Load Index

6.2.3 Free Bending

TABLE 9: MP2 program - Free bending

FIGURE 18: Comparison of calculated and measured burst pressures in free bending (MP-2 data)

6.2.4 Restrained Bending

TABLE 10: MP2 program - Restrained bending

STEP	TIME	DISP	FORCE	MOMENT	ROTATION	REACT	REACT	REACT	REACT
------	------	------	-------	--------	----------	-------	-------	-------	-------

FIGURE 19: Comparison of calculated and measured burst pressures in restrained bending (MP-2 data)

6.3 Westinghouse Data

Tests were performed by Westinghouse in 1989 through 1992 for several US and Spanish plants (ref. 10). Seventy six experimental data are compared to the calculated values. The results are considered separately for free bending and supported configurations. Six additional data points with Multiple Circumferential Indications (MCI) are not included because the corresponding calculation formula have not been developed in the present report; lumping the total defect area in a single through-wall segment would have been unduly conservative for the purpose of this report.

6.3.1 Testing conditions

The test specimens were manufactured from 3/4" ($t = 0.043$ ") and 7/8" ($t = 0.05$ ") diameter tubes, with 100% through-wall flaws. A plastic bladder and local foil reinforcement was used to prevent leakage.

The flaws were located at a short distance above a simulated tube sheet. Free bending was either allowed or prevented by lateral restraint.

Various test support configurations were used. The support configurations simulated the presence of one or two tube support plates at 8", 27.5" and 49.75" above TTS. In some cases the axial tube movement was also prevented (clamped configuration).

6.3.2 Load Index

6.3.3 Free Bending

TABLE 11: Westinghouse program - Free bending ($R/t = 8.24$)



FIGURE 20: Comparison of calculated and measured burst pressures in free bending (Westinghouse data)

6.3.4 Restrained Bending

TABLE 12: Westinghouse program - Restrained bending ($R/t=8.24$)

FIGURE 21: Comparison of calculated and measured burst pressures in restrained bending (Westinghouse data)

6.4 ANO-2 Data

Test were performed by Combustion Engineering in 1995 for unit 2 of the Arkansas Number One (ANO-2) plant of Entergy Operations (ref.11). Most of the samples had laboratory corrosion cracks (LCC); a pulled tube (PUL) was also burst tested and compared to several EDM flaws approximating the same morphology. Forty four experimental data are compared to the calculated values.

6.4.1 Testing Conditions

The test specimens were manufactured from 3/4" ($t = 0.048$ ") diameter tubes. Test specimens had partial penetration and through-wall flaws. A plastic bladder, without foil reinforcement was used to prevent leakage.

The flaws were located 1.6 mm above a simulated tube sheet. Free bending was prevented by lateral restraint. The support configurations simulated the presence of one egg crate at 27" above TTS . However, for most of the tests, the PDA was low enough to initiate axial burst which is not dependent on the support presence.

The testing procedure did not comply with the intent of the EPRI burst test guidelines (ref. 8), as the lack of foil reinforcement may prevent to achieve true burst in a large proportion of the tests.

6.4.2 Load Index

6.4.3 Data

TABLE 13: ANO2 data - Restrained bending ($R/t=7.31$ and $\kappa=0.65$)

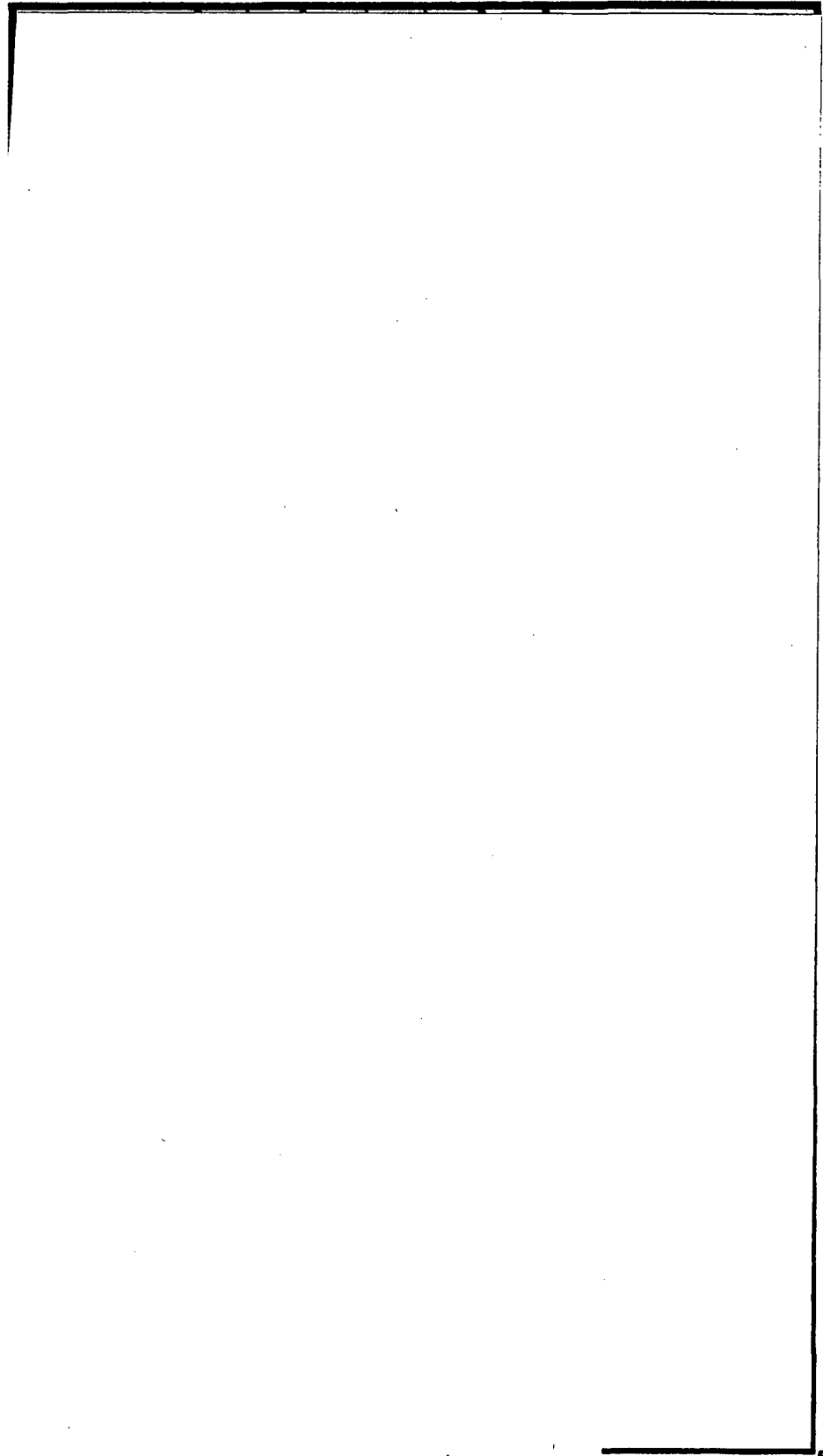


FIGURE 22: Comparison of calculated and measured burst pressures (ANO-2 data)

6.5 Framatome Data

Tests were performed by Framatome in the eighties on EDM samples (ref. 7). Forty two burst data were obtained; however only the average values are reported for each of the 12 different tested configurations. These are compared to the calculated values. The results are considered separately for free bending and supported configurations.

6.5.1 Testing Conditions

The test specimens were manufactured from 7/8" ($t = 0.05$ ") diameter tubes, with 100% through-wall flaws. A plastic bladder and local foil reinforcement was used to prevent leakage.

The flaws were located 75 mm (3") above a simulated tube sheet. Free bending was either allowed or prevented by lateral restraint.

The support configurations simulated the presence of one tube support plate at 0.15 m (6"), 0.5 m (20") or 1 m (40") above TTS . Most of the tests used the shortest distance.

6.5.2 Load Index

6.5.3 Free Bending

TABLE 14: Framatome program - Free bending

FIGURE 23: Comparison of calculated and measured burst pressures in free bending (averages of 10 Framatome data)

6.5.4 Restrained Bending

TABLE 15: Framatome program - Restrained bending

FIGURE 24: Comparison of calculated and measured burst pressures in restrained bending (averages of 32 Framatome data points)

6.6 EDF Data (Pulled Tubes)

EDF has performed extensive burst testing of tubes pulled from French SG affected by circumferential cracking from either PWSCC (13 data) or ODSCC (28 data); these results are presented in ref.12.

Unfortunately the tests were performed without simulated lateral support and do not comply with the EPRI guidelines (ref. 8); a wide foil of high strength alloy (UTS > 1000 MPa) was bonded in the tube and true burst was not always achieved (undocumented in ref.12).

While these tests provide crucial insight on the remaining strength of real degraded tubes, they cannot be used reliably to support or verify a quantitative assessment tool.

6.7 Conclusions

6.7.1 Free Bending

When all free bending data (excluding axial burst) are considered together, the following behavior is systematically observed:

FIGURE 25: Comparison of calculated and measured normalized burst pressures (all data except free bending)

6.7.3 Validation

These results appear particularly meaningful when considering the large variation in testing parameters. The tests were conducted by four independent testing laboratories (Laborelec, Westinghouse, CE and Framatome) and involved two major testing procedures ("weak" and "strong" foil). Two tube sizes (3/4" and 7/8" ϕ) and two ratios of mean radius to wall thickness (8.24 and 7.31) were tested. Over ten lateral restraint configurations simulating various combinations of flow distribution baffles, tube support plates, and egg crate supports were employed in the tests. The tested flaw morphologies (EDM notches and real cracks) consisted of partial penetration flaws and through-wall flaws, with or without wall penetration over the remaining circumference. The main flaw length ranged from 0° to 300°, and tube support lateral restraint offset ranged from 0 to 20 mm.

The available data base provides a comprehensive validation support for the analytical model. There is no strong need to extend this data base for the sole purpose of further validation. However it is recommended that other existing or future burst test results should be evaluated for inclusion in the data base, subject to a sufficient degree of compliance with the relevant testing guidelines (ref. 8).

7 PROPOSED SGDSM IMPLEMENTATION

7.1 Generic approach

The following approach is suggested to address circumferentially flawed tubes under Steam Generator Defect Specific Management (SGDSM).

A simple and conservative approximation is obtained by using the following assumptions:

FIGURE 26: Bending and tensile components of the reference curve

FIGURE 27: Failure modes considered by the reference curve

FIGURE 28: Sensitivity of the reference curve to variations of the R/t ratio

FIGURE 29: Reference curve as a lower bound of the expected failure area

FIGURE 30: Linear approximation of the reference curve

7.2 Alternate Repair Limit

7.2.1 Structural limit

TABLE 16: Typical reference pressures

FIGURE 31: Definition of the structural limit

7.2.2 Repair Limit

Two important corrective terms, PDA_{NDE} and PDA_{CG} , are required to derive the Begin Of Cycle (BOC) allowable PDA..

PDA_{NDE} depends on the inspection technique and, more specifically, on the detection sensitivity and the sizing accuracy for the specific defect morphology. A conservative envelope value of the real flaw size can be obtained by correcting the measured depth value over the detected length and by adding the depth detection threshold over the remaining part of the circumference.

PDA_{CG} depends on the material susceptibility, defect morphology, local stress conditions and cycle operating conditions (temperature, fluid chemistry, concentration processes, etc.). It may also depend on the cycle length and the BOC flaw size.

The determination of parameters PDA_{NDE} and PDA_{CG} is beyond the scope of this report and may need site specific developments.

7.3 Tube Rupture Probability

The following approach is proposed for determining the probability of tube rupture with circumferential flaws present. The reference curve is considered as a conservative lower bound, not associated with any uncertainty. The Steam Generator Tube Rupture (SGTR) probability is then calculated as the combined probability of exceeding the reference curve for the given differential pressure and the statistical distributions of:

- the flaw PDA sizes at BOC (inspection data)
- the NDE sizing uncertainty
- the PDA growth rate
- the high temperature mechanical properties ($\sigma_u + \sigma_y$)
- the ratio R/t (if available)

This approach is somewhat conservative but has the major advantage of avoiding the need to develop an uncertainty model for the burst pressure correlation. This may be difficult because of the many test variables (cf. Section 7.6). The approach also has the advantage of allowing efforts to be concentrated on the two areas of concern which are really challenging the industry: NDE detection and sizing uncertainty, and crack growth uncertainty.

7.4 Accident Leak Rate

The structural model proposed in this report has a physical basis which lends itself well to a simple calculation of deformations and, more particularly, flaw leakage areas. This allows a leakage rate model to be constructed in a way consistent with that established for axial cracks and documented in EPRI report NP 6864-L (ref. 14). Such an approach is documented in a companion report (ref. 15).

7.5 Plant Specific Approach

A less conservative approach may be used by defining an "adjusted reference curve" based on plant specific features:

- lowest stiffness index value applicable to the particular lateral restraint design
- crack morphology (in case of OD initiation)
- high temperature LTL value of ($\sigma_u + \sigma_y$) for the tubes actually used .

FIGURE 32: Reference curve adjusted to plant specific data

7.6 Comparison to the Empirical Correlation Approach

8 MODEL CONSERVATISM

8.1 Thin Wall Approximation

8.2 Defect Morphology

8.2.1 Shape of Degraded Area

8.2.2 Out of Plane Components

8.2.3 Leakage Correlation

8.3 Restraint Configuration

8.4 Pressure Load on Flaw Lips

8.5 Ligaments in Crack Lips

8.6 Failure Stress in Tensile Mode

9 Overall Comparison with Burst Data

All normalized burst data (except for the non relevant free bending cases) have been plotted in figure 33 for comparison with the reference curve and predicted failure area. The data have been approximately adjusted to a load index $\eta = -0.5$, by a 30% reduction when obtained with a "strong foil procedure" and a 15% reduction (average of the expected 0-30 % range) for some MP-2 tests (series D) using a non qualified testing procedure. Four tensile tests (Belgian program) on pulled tubes have been translated into equivalent pressures. Three data on unflawed tubes (ANO-2 program) have been omitted.

A large scatter is apparent, with most data points well above the reference curve. This large scatter is due to the various testing configurations (symmetry, restraint type and location, ligaments, etc.) and the inherent correlation uncertainty.

FIGURE 33: Location of normalized burst data with respect to reference curve (all data except free bending)

According to the theoretical predictions, all data points should be contained within the failure area, as defined in figure 29. Small deviations outside of this area

FIGURE 34: Location of normalized burst data with respect to reference curve (differentiated by failure mode)

FIGURE 35: Location of normalized burst data with respect to reference curve (differentiated by flaw types)

10 UTILITY GUIDANCE

The structural model and analysis described in this report may be used by the Utilities, either directly or through their contractors and consultants, to achieve one or both of the following objectives:

- 1) Implement a SGDSM policy for circumferential cracking. This involves standard procedures for "condition monitoring" and "operational assessment". Sections 10.1 and 10.2 describe how to define the structural and repair limits. The complementary assessments of SGTR probability and of accident leakage need some further development, along the lines of Sections 7.3 and 7.4.
- 2) Perform a "detailed condition monitoring", when required for some particular flawed tubes. This involves a complete structural analysis on basis of the full modeling capabilities, as described in Section 10.3.

The main procedural steps are summarized hereafter and provide guidance to the more detailed information contained in this report.

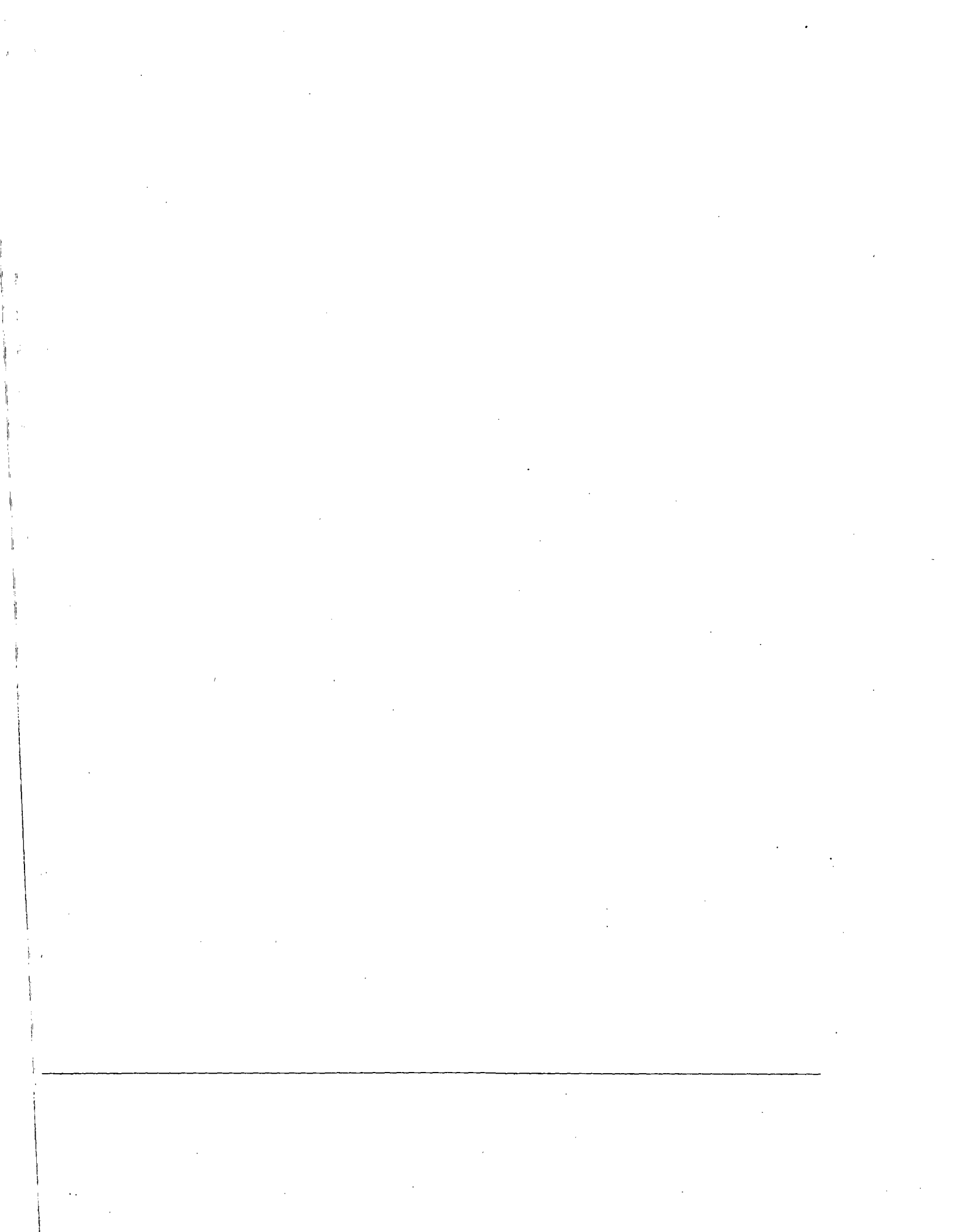
10.1 Structural Limit

The structural PDA limit may be defined on basis of either a generic or specific approach.

The generic approach is usually more conservative; it uses predefined lower bound procedures and requires little additional calculation.

The specific approach takes advantage of plant specific data to reduce the amount of conservatism, while still complying with the RG 1.121 requirements; it requires development, justification and documentation of the procedures to be used.

10.1.1 Generic Approach



10.1.2 Specific Approach

10.2 Repair Limit

10.3 Detailed Condition Monitoring

11 SUMMARY and CONCLUSIONS

A structural analysis model has been developed that allows a simple yet accurate prediction of the burst pressure of tubes degraded by circumferential flaws, under either laboratory testing or actual SG service conditions. The model and associated methodology is an extension of the well known net section collapse load approach. The model accounts for the bending, tensile or axial failure modes, ligaments in the main flaw, and wall penetration outside of the main flaw. The model also addresses various lateral restraint configurations, the effect of reinforcing foils used for laboratory burst tests of through-wall defects, and the effect of fluid pressure acting on the crack lips under normal operating or accident conditions.

Over 250 burst data from four independent laboratories have been compared and shown to be consistent with the predicted values from the model. This comprehensive integrated data base provides an adequate and sufficient validation support.

The derived structural model was used to determine a lower bound correlation between the normalized burst pressure and the Percentage Degraded Area (PDA) for actual SG conditions. This "reference curve" is proposed for SGDSM implementation in SG of Westinghouse and CE design, on basis of the following conservative assumptions:

- 1) total circumferential flaw area lumped in the most unfavorable configuration: either a single 100 % through-wall segment or a symmetrical ID flaw.
- 2) half the differential pressure acting on the lips of the through-wall defect or full pressure acting on the symmetrical flaw.
- 3) mechanical properties (650°F) at their Lower Tolerance Limit (LTL at 95/95 % confidence level).
- 4) lowest lateral restraint stiffness.

Alternatively, plant specific data (flaw initiation side, mechanical properties and/or restraint stiffness) may be taken into account, resulting in a less conservative "adjusted reference curve".

A detailed evaluation of the various underlying conservatisms does not show excessive margins. The overall approach should therefore not be considered as over conservative.

A major feature of the "reference curve" approach is that the circumferential flaw is entirely defined by a single parameter: the degraded area expressed as a % of the full tube cross section, which can be indifferently called PDA or average flaw depth. Consequently the NDE flaw characterization must be aimed at that parameter in all respects of detection, sizing and growth.

The reference curve can be used for both the definition of a structural limit, leading to an alternate repair limit, and the calculation of Steam Generator Tube Rupture (SGTR) probability.

Utility guidance is provided to achieve the two main objectives of the structural model and analysis:

- 1) Implementation of a SGDSM policy
- 2) Performance of a "detailed condition monitoring", when required for some particular degraded tubes.

It is concluded that the structural analysis of circumferentially flawed tubes is well under control and that the real remaining issue is restricted to the uncertainties affecting the NDE detection and sizing techniques and the knowledge of in service growth rates. Subject to a satisfactory resolution of these concerns, there is no reason why circumferential flaws should not be allowed to remain safely in service, when complying with a repair limit defined under the generic SGDSM methodology.

REFERENCES

1. "Evaluation of Flaws in Austenitic Steel Piping", report of "Section XI Task Group for Piping Flaw Evaluation, ASME Code", Journal of Pressure Vessel Technology, Vol. 108, August 1986.
2. Schulze, G. Toggler and E. Bodmann, "Fracture Mechanics Analysis on the Initiation and Propagation of Circumferential and Longitudinal Cracks in Straight Pipes and Pipe Bends", NED 58, 1980.
3. "A Methodology for Structural Assessment of SG Tubes with Complex and Multiple Circumferential flaws", N. Cofie (Structural Integrity Associates), presented at the EPRI ARC committee meeting, Chicago, May 1995.
4. "Circumferential Cracks in Steam Generator Tubes: Burst Pressure Testing / Evaluation of Foil Reinforcement Effects", EPRI Final Report Volume 2, TR-107618, December, 1997.
5. "Belgian Approach to Steam Generator Tube Plugging for PWSCC", EPRI report NP-6626-SD and its addendum "Experimental Work", March 1990.
6. "Burst Pressure Correlation for SG Tubes with Through wall Axial Cracks", prepared by Westinghouse, Laborelec and Packer Engineering, February 1995.
7. "Steam Generator Tube Integrity - Volume 1: Burst test results and validation of rupture criteria (Framatome data)", EPRI report NP-6865-L, June 1991.
8. "EPRI Guidelines for Burst Testing of Steam Generator Tubes", prepared by Westinghouse, Laborelec and Packer Engineering, July 1994.
9. "Summary of Nuclear Materials and Chemistry's Millstone 2 Steam Generator Tube Related Burst test Programs", Northeast Utilities memorandum NMC-91-103, May 1991.
10. Private Communications with Westinghouse transmitting data documented in reports SG-89-12-004 (ASCO, December 1989), WCAP-13034 (North Anna 1, August 1991), and WCAP-13326 (April 1992).
11. "ANO Unit 2 Steam Generator Tubes Evaluation of Burst Pressures with Circumferential Flaws Present", Tetra Engineering Group report TR-95-024, April 11, 1996
12. "Circumferential cracking at the top of the tube sheet - Results of pulled tubes examinations", F. Cattant, EdF report presented at the EPRI workshop on circumferential cracking of SG tubes, Charlotte, June 1995.

13. "Inconel Alloy 600 Tubing Material Burst and Strength Properties", Westinghouse report WCAP-12522, January 1990.
14. "PWR Steam Generator Tube Repair Limits: Technical Support Document for Expansion Zone PWSCC in Roll Transitions", EPRI report NP-6864-L, Revision 2, August 1993.
15. "Circumferential Cracks in Steam Generator Tubes: Leak Rate Analysis", EPRI Final Report Volume 3, TR-107618, December, 1997.

APPENDIX A - Development and resolution of equations

A1 Equilibrium Equations

A2 Analytical Resolution

A3 Numerical Resolution

A4 Calculation Results

A5 Specificity of EDM flaws

TABLE A1 - Through-wall flaw in free bending

TABLE A2 - Through-wall flaw in restrained bending ($\kappa = 0.6$)

TABLE A3 - Through-wall flaw in restrained bending ($\kappa = 0.7$)

TABLE A4 - Through-wall flaw in restrained bending ($\kappa = 0.8$)

TABLE A5 - Through-wall flaw in restrained bending ($\kappa = 0.9$)

TABLE A6 - Partial penetration flaw in free bending

TABLE A7 - Partial penetration flaw in restrained bending ($\kappa=0.6$)

TABLE A8 - Partial penetration flow in restrained bending ($\kappa=0.7$)

TABLE A9 - Partial penetration flaw in restrained bending ($\kappa=0.8$)

TABLE A10 - Partial penetration flaw in restrained bending ($\kappa=0.9$)

TABLE A11 Symmetrical flow

APPENDIX B - Lateral restraint stiffness

B1 Scope

B2 Beam Model

B3 Subcase 1

B5 Combined Case

B6 Single Lateral Restraint

B7 Flaw Located at Mid Span

B8 Tube Clamping in Second Lateral Restraint

RESULTS

This report consists of three volumes. The first volume defines a structural analysis method for assessing the residual strength, that is the burst susceptibility of steam generator tubes affected by circumferential cracking at the tube expansion zone. The structural analysis accounts for the total degraded cross sectional area as the primary functional parameter and redistributes this area in the most conservative manner related to structural integrity. The analysis accounts for the tube lateral restraint provided by the tubesheet and tube support plates. It also considers the effect of pressure load on the degradation's crack lips and the restraining load from foil reinforcement used in laboratory burst testing of tube specimens used in developing necessary correlations. The latter effect of foil reinforcement is discussed in volume 2 of this report. Finally, volume 3 defines and justifies a leak rate model for circumferential cracks at the expansion zone. The leakage model is the same as previously used for axial cracks produced by PWSCC.

EPRI PERSPECTIVE

This report defines a structural and leakage integrity model for assessing steam generator tubes affected by circumferential cracks at the tube expansion zone. The structural model is an improved version of that described in EPRI Report NP-6626-SD, Belgian Approach to Steam Generator Tube Plugging for PWSCC, March 1990. The leakage model is the same as previously developed for axial cracking as documented in EPRI Report NP-6864-L-Rev. 2, PWR Steam Generator Tube Repair Limits: Technical Support Document for Expansion Zone PWSCC in Roll Transitions, August 1993. A further refined ARC for circumferential cracking than that presented in this report is presented in EPRI Interim Technical Report, TR-107197, Depth Based Structural Analysis Methods for SG Circumferential Indications, November 1997.

TR-107618

INTEREST CATEGORY:

Steam Generators

KEY WORDS:

Nuclear Steam Generators

Material Degradation

Reliability

REPORT SUMMARY

CIRCUMFERENTIAL CRACKS IN STEAM GENERATOR TUBES: STRUCTURAL ANALYSIS MODEL AND INTEGRATED BURST PRESSURE DATA BASE

The Ad-hoc Alternate Repair Committee of the Steam Generator Management Program initiated work in the area of corrosion induced circumferential cracking in steam generator tubes. The intent of the effort is to develop information that can be used to develop an alternate repair criteria (ARC) for tubes exhibiting this form of degradation at the steam generator tubesheet location. Initial work performed early in the investigative process to develop the ARC is documented in three volumes of this report.

BACKGROUND

Circumferential cracking in steam generator tubes exists in the tubesheet expansion zone. Such cracking is difficult to accurately size and compare to a plant's technical specification depth based repair limit. In many cases this comparison requires the affected tube to be repaired even though it's structural and leakage integrity have not been compromised. To help utilities avoid unnecessary repair, the EPRI Steam Generator Management Program through the Ad-hoc Alternate Repair Committee focused on developing an alternate repair limit for circumferential cracking justified by existing laboratory and field data in conjunction with appropriate conservative assumptions.

OBJECTIVE

To provide technical support documents that may be used in justifying repair limits for tubes exhibiting circumferential cracking in steam generator roll expansion zones.

APPROACH

To develop an alternate tube repair criteria for circumferential cracking which builds on previous work developed for justifying structural and leakage integrity of steam generator tubes experiencing primary water stress corrosion cracking (PWSCC) at roll expansion zones.



Export Control Restrictions

Access to and use of EPRI Intellectual Property is granted with the specific understanding and requirement that responsibility for ensuring full compliance with all applicable U.S. and foreign export laws and regulations is being undertaken by you and your company. This includes an obligation to ensure that any individual receiving access hereunder who is not a U.S. citizen or permanent U.S. resident is permitted access under applicable U.S. and foreign export laws and regulations. In the event you are uncertain whether you or your company may lawfully obtain access to this EPRI Intellectual Property, you acknowledge that it is your obligation to consult with your company's legal counsel to determine whether this access is lawful. Although EPRI may make available on a case by case basis an informal assessment of the applicable U.S. export classification for specific EPRI Intellectual Property, you and your company acknowledge that this assessment is solely for informational purposes and not for reliance purposes. You and your company acknowledge that it is still the obligation of you and your company to make your own assessment of the applicable U.S. export classification and ensure compliance accordingly. You and your company understand and acknowledge your obligations to make a prompt report to EPRI and the appropriate authorities regarding any access to or use of EPRI Intellectual Property hereunder that may be in violation of applicable U.S. or foreign export laws or regulations.

About EPRI

EPRI creates science and technology solutions for the global energy and energy services industry. U.S. electric utilities established the Electric Power Research Institute in 1973 as a nonprofit research consortium for the benefit of utility members, their customers, and society. Now known simply as EPRI, the company provides a wide range of innovative products and services to more than 1000 energy-related organizations in 40 countries. EPRI's multidisciplinary team of scientists and engineers draws on a worldwide network of technical and business expertise to help solve today's toughest energy and environmental problems.

EPRI. Electrify the World

SINGLE USER LICENSE AGREEMENT

THIS IS A LEGALLY BINDING AGREEMENT BETWEEN YOU AND THE ELECTRIC POWER RESEARCH INSTITUTE, INC. (EPRI). PLEASE READ IT CAREFULLY BEFORE REMOVING THE WRAPPING MATERIAL.

BY OPENING THIS SEALED PACKAGE YOU ARE AGREEING TO THE TERMS OF THIS AGREEMENT. IF YOU DO NOT AGREE TO THE TERMS OF THIS AGREEMENT, PROMPTLY RETURN THE UNOPENED PACKAGE TO EPRI AND THE PURCHASE PRICE WILL BE REFUNDED.

1. GRANT OF LICENSE

EPRI grants you the nonexclusive and nontransferable right during the term of this agreement to use this package only for your own benefit and the benefit of your organization. This means that the following may use this package: (I) your company (at any site owned or operated by your company); (II) its subsidiaries or other related entities; and (III) a consultant to your company or related entities, if the consultant has entered into a contract agreeing not to disclose the package outside of its organization or to use the package for its own benefit or the benefit of any party other than your company.

This shrink-wrap license agreement is subordinate to the terms of the Master Utility License Agreement between most U.S. EPRI member utilities and EPRI. Any EPRI member utility that does not have a Master Utility License Agreement may get one on request.

2. COPYRIGHT

This package, including the information contained in it, is either licensed to EPRI or owned by EPRI and is protected by United States and international copyright laws. You may not, without the prior written permission of EPRI, reproduce, translate or modify this package, in any form, in whole or in part, or prepare any derivative work based on this package.

3. RESTRICTIONS

You may not rent, lease, license, disclose or give this package to any person or organization, or use the information contained in this package, for the benefit of any third party or for any purpose other than as specified above unless such use is with the prior written permission of EPRI. You agree to take all reasonable steps to prevent unauthorized disclosure or use of this package. Except as specified above, this agreement does not grant you any right to patents, copyrights, trade secrets, trade names, trademarks or any other intellectual property, rights or licenses in respect of this package.

4. TERM AND TERMINATION

This license and this agreement are effective until terminated. You may terminate them at any time by destroying this package. EPRI has the right to terminate the license and this agreement immediately if you fail to comply with any term or condition of this agreement. Upon any termination you may destroy this package, but all obligations of nondisclosure will remain in effect.

5. DISCLAIMER OF WARRANTIES AND LIMITATION OF LIABILITIES

NEITHER EPRI, ANY MEMBER OF EPRI, ANY COSPONSOR, NOR ANY PERSON OR ORGANIZATION ACTING ON BEHALF OF ANY OF THEM:

- (A) MAKES ANY WARRANTY OR REPRESENTATION WHATSOEVER, EXPRESS OR IMPLIED, (I) WITH RESPECT TO THE USE OF ANY INFORMATION, APPARATUS, METHOD, PROCESS OR SIMILAR ITEM DISCLOSED IN THIS PACKAGE, INCLUDING MERCHANTABILITY AND FITNESS FOR A PARTICULAR PURPOSE, OR (II) THAT SUCH USE DOES NOT INFRINGE ON OR INTERFERE WITH PRIVATELY OWNED RIGHTS, INCLUDING ANY PARTY'S INTELLECTUAL PROPERTY, OR (III) THAT THIS PACKAGE IS SUITABLE TO ANY PARTICULAR USER'S CIRCUMSTANCE; OR
- (B) ASSUMES RESPONSIBILITY FOR ANY DAMAGES OR OTHER LIABILITY WHATSOEVER (INCLUDING ANY CONSEQUENTIAL DAMAGES, EVEN IF EPRI OR ANY EPRI REPRESENTATIVE HAS BEEN ADVISED OF THE POSSIBILITY OF SUCH DAMAGES) RESULTING FROM YOUR SELECTION OR USE OF THIS PACKAGE OR ANY INFORMATION, APPARATUS, METHOD, PROCESS OR SIMILAR ITEM DISCLOSED IN THIS PACKAGE.

6. EXPORT

The laws and regulations of the United States restrict the export and re-export of any portion of this package, and you agree not to export or re-export this package or any related technical data in any form without the appropriate United States and foreign government approvals.

7. CHOICE OF LAW

This agreement will be governed by the laws of the State of California as applied to transactions taking place entirely in California between California residents.

8. INTEGRATION

You have read and understand this agreement, and acknowledge that it is the final, complete and exclusive agreement between you and EPRI concerning its subject matter, superseding any prior related understanding or agreement. No waiver, variation or different terms of this agreement will be enforceable against EPRI unless EPRI gives its prior written consent, signed by an officer of EPRI.

TR-107618-V1

© 1997 Electric Power Research Institute (EPRI), Inc. All rights reserved. Electric Power Research Institute and EPRI are registered service marks of the Electric Power Research Institute, Inc. EPRI. ELECTRIFY THE WORLD is a service mark of the Electric Power Research Institute, Inc.

♻️ Printed on recycled paper in the United States of America